Hearing Research 457 (2025) 109170

Contents lists available at ScienceDirect

Hearing Research

journal homepage: www.elsevier.com/locate/heares

Extent of genetic and epigenetic factor reprogramming via a single viral vector construct in deaf adult mice

Niliksha Gunewardene [a,b], Patrick Lam [a], Jiwei Song [a], Trung Nguyen [a], Shannon Mendez Ruiz [d,e], Raymond C.B. Wong [d,e], Andrew K. Wise [a,b,c,1], Rachael T. Richardson [a,b,c,1,*]

[a] Bionics Institute, East Melbourne, Victoria 3002, Australia
[b] Department of Medical Bionics, The University of Melbourne, Fitzroy, Victoria 3065, Australia
[c] Department of Surgery (Otolaryngology), University of Melbourne, The Royal Victorian Eye and Ear Hospital, East Melbourne, Victoria 3002, Australia
[d] Centre for Eye Research Australia, Royal Victorian Eye and Ear Hospital, East Melbourne, Victoria, Australia
[e] Ophthalmology, Department of Surgery, University of Melbourne, East Melbourne, Victoria, Australia

ARTICLE INFO

Keywords:
Atoh1
Epigenetic factors
Gene therapy
Hair cell
Regeneration
Hearing loss
Cochlea

ABSTRACT

In the adult mammalian cochlea, hair cell loss is irreversible and causes deafness. The basic helix-loop transcription factor Atoh1 is essential for normal hair cell development in the embryonic ear. Over-expression of Atoh1 in the adult cochlea by gene therapy can convert supporting cells (cells that underlie hair cells) into a hair cell lineage. However, the regeneration outcomes can be inconsistent. Given that hair cell development is regulated by multiple signalling and transcriptional factors in a temporal and spatial manner, a more complex combinatorial approach targeting additional transcription factors may be required for efficient hair cell regeneration. There is evidence that epigenetic factors are responsible for the lack in regenerative capacity of the deaf adult cochlea. This study aimed to develop a combined gene therapy approach to reprogram both the genome and epigenome of supporting cells to improve the efficiency of hair cell regeneration. Adult Pou4f3-DTR mice were used in which the administration of diphtheria toxin was used to ablate hair cells whilst leaving supporting cells relatively intact. A single adeno-associated viral construct was used to express human Atoh1, Pou4f3 and short hairpin RNA against Kdm1a (regeneration gene therapy) at two weeks following partial or severe hair cell ablation. The average transduction of the inner supporting cells, as measured by the control AAV2.7m8-GFP vector in the deaf cochlea, was only 8 % while transduction in the outer sensory region was <1 %. At 4- and 6-weeks post-treatment the number of Myo+ hair cells in the control and regeneration gene therapy-treated mice were not significantly different. Of note, although both control and regeneration gene therapy treated cochleae contained supporting cells that co-expressed the hair cell marker Myo7a and the supporting cell marker Sox2, the regeneration gene therapy treated cochleae had significantly higher numbers of these cells ($p < 0.05$). Furthermore, among these treated cochleae, those that had more hair cell loss had a higher number of Myo7a positive supporting cells (R2=0.33, Pearson correlation analysis, $p < 0.001$). Overall, our results indicate that the adult cochlea possesses limited intrinsic spontaneous regenerative capacity, that can be further enhanced by genetic and epigenetic reprogramming.

1. Introduction

A major cause of deafness is the loss of the sensory hair cells in the cochlea. Unfortunately, hair cells do not spontaneously regenerate in the mammalian adult ear (Fujioka et al., 2015; Groves, 2010), and thus the hearing loss that results from hair cell damage is essentially irreversible. Conversely, in some lower vertebrates such as birds and fish, spontaneous hair cell regeneration and functional recovery can be achieved in the cochlea following hair cell loss (Corwin and Cotanche, 1988; Ryals and Rubel, 1988; Cotanche et al., 1994; Adler and Raphael, 1996). The supporting cells residing underneath the hair cells re-enter the cell cycle or trans-differentiate to produce new hair cells. This discovery led to a

* Corresponding author.
E-mail address: rrichardson@bionicsinstitute.org (R.T. Richardson).
[1] Co-last authors.

https://doi.org/10.1016/j.heares.2024.109170
Received 23 July 2024; Received in revised form 9 December 2024; Accepted 17 December 2024
Available online 20 December 2024

surge in research focused on understanding the underlying mechanism of regeneration in lower vertebrates and the quest for novel strategies to promote mammalian hair cell regeneration using genetic or pharmacological therapies.

The basic helix-loop transcription factor Atoh1 is essential and necessary for normal hair cell development in the embryonic ear (Bermingham et al., 1999). Considerable evidence has revealed that in vitro overexpression of Atoh1 in cochlear explants can reprogram non-sensory cells of the inner ear into hair-cell-like cells (Zheng and Gao, 2000; Shou et al., 2003). Ectopic expression of Atoh1 in neonatal mice led to robust conversion of supporting cells into hair cell-like cells, but this regenerative capacity rapidly declined with age (Liu et al., 2012; Kelly et al., 2012). This age-related decline can be attributed to epigenetic changes caused by the accumulation of chemical changes on DNA or histones causing hair cell loci to become epigenetically inaccessible with the morphology of the chromatin changing from a euchromatin to heterochromatin state (Jen et al., 2019; Tao et al., 2021; Iyer et al., 2022). In the deaf adult cochlea, adenoviral expression of Atoh1 promoted some hair cell regeneration, but hearing restoration was variable or negligible (Izumikawa et al., 2005; Atkinson et al., 2014), potentially due to insufficient numbers of new hair cells and/or poor functional maturation of the newly regenerated hair cells. Given that hair cell development is regulated by multiple signalling and transcriptional factors in a temporal and spatial manner, expression of Atoh1 alone in residual supporting cells may not be sufficient for efficient hair cell generation, emphasising the need for a more complex combinatorial approach targeting additional transcription factors and/or chromatin modifying enzymes.

There have now been multiple transcription factors tested in combination with Atoh1 to promote hair cell generation and maturation. The two most targeted transcription factors include Pou4f3 and Gfi1. Pou4f3 is a downstream target gene of Atoh1 implicated to promote hair cell survival and function during normal hair cell development (Ikeda et al., 2015). Gfi1, a zinc finger transcription factor necessary for differentiation and survival of hair cells, is a target of Pou4f3 (Hertzano et al., 2004). It is upregulated during early hair cell development and its expression is maintained in differentiating and immature hair cells (Wallis et al., 2003). Recent evidence suggests that both Gfi1 and Pou4f3 interact with Atoh1 to regulate hair cell differentiation. Pou4f3 increases the accessibility of Atoh1 target genes by driving Atoh1 to bind and drive their expression, while Gfi1 regulates hair cell differentiation by acting as an off-DNA transcriptional co-activator of Atoh1 (Jen et al., 2022). In vitro and in vivo studies revealed that co-expression of one or more of Gfi1 and Pou4f3 with Atoh1 was more effective at promoting hair cell reprogramming, compared to Atoh1 alone (Costa et al., 2015; Walters et al., 2017; Chen et al., 2021; McGovern et al., 2024). Adenoviral delivery of Atoh1 and Gfi1 in the one construct to deaf adult mice also resulted in improved regeneration through supporting cell transdifferentiation at improved efficiency compared to Atoh1 alone (Lee et al., 2020). However, the functional recovery of hearing thresholds has yet to be reported with these combinatorial approaches.

Epigenetic modifications including DNA methylation and histone modifications are implicated as a potential factor for the decline in regenerative capacity in the adult cochlea (Jen et al., 2019; Tao et al., 2021; Nguyen et al., 2023). Target genes necessary for the differentiation of supporting cells to hair cells become inaccessible to transcription factor networks as heterochromatin and repressive modifiers inhibit genes required for hair cell maturation (Samarajeewa et al., 2018). Simultaneous comparison of the transcriptome and epigenome of supporting cells and non-sensory cells of early postnatal mice show that hair cell loci become progressively less epigenetically accessible from birth to 1 week of age (Iyer et al., 2022). Furthermore, it was shown that despite the overexpression of the three genes Atoh1, Pou4f3 and Gfi1 in improving the number of hair cells generated (compared to Atoh1 treatment alone), the transcriptional profile of "new" hair cells remained immature. Here it needs to be noted that the above study used early postnatal mice and the transcriptional profile could differ in the deaf adult animal in response to the three-factor combination.

Accumulating evidence indicates that epigenetic reprogramming improves regeneration outcomes in multiple systems including the eye (Lu et al., 2020), spinal cord (Muller et al., 2022), and heart (Kurotsu et al., 2017), to name a few. In the cochlea, the combination of epigenetic drugs that target chromatin modifying enzymes including HDAC, Lsd1 or EZH2 with drugs that activate Atoh1 via the Notch or Wnt signaling pathways potentiated hair cell regeneration, above what could be achieved with Atoh1 activation only (Tao et al., 2021; Lenz et al., 2019; McLean et al., 2017). In the current study, we sought to address if the combination of genetic and epigenetic targeting would improve hair cell regeneration outcomes. Here, we aimed to test if adeno-associated viral delivery of hAtoh1, hPou4f3 and short hairpin RNA (*sh*RNA) targeting Kdm1a (encodes Lsd1) would improve the responsiveness of supporting cells to hair cell gene activation. There is evidence in the neonatal mouse cochlea that Lsd1 inhibition using a drug GSK extends the duration of transdifferentiation capacity of supporting cells between postnatal day 1–3 (Tao et al., 2021). Furthermore, in other systems, Lsd1 depletion is associated with the upregulation of Gfi1 mediated by a loss in HDAC activity (Kerenyi et al., 2013; Maiques-Diaz and Somervaille, 2016; Maiques-Diaz et al., 2018). Given the risk of off-target effects previously reported for epigenetic drugs and their lack of specificity (Holtzman and Gersbach, 2018), we chose to selectively modify the epigenome using AAV by testing *sh*RNA mediated Lsd1 repression.

Despite seeing no significant change in overall hair cell density compared to control, there was a substantial number of cells that expressed the hair cell genes post-regeneration gene therapy (Regen) treatment that co-localised with supporting cell and hair cell markers indicating the generation of "new" hair cell-like cells. Of note, in a small cohort of mice that were completely deaf, hAtoh1 expressing cells were detected, indicating the potential to reactivate hair cell developmental genes even in a severely damaged sensory epithelium usually considered unresponsive to regeneration. To the best of our knowledge, this is the first study to evaluate the impact of genetic and epigenetic reprogramming in the deaf adult cochlea.

2. Methods

2.1. Experimental animals

We used both male and female adult heterozygous Pou4f3-DTR mice (C57BL/6 J background), kindly provided by Prof Edwin Rubel (University of Washington, Seattle), in which deafness can be induced by injection of diphtheria toxin (DT; Sigma-Aldrich) (Tong et al., 2015). The mice were 4–6 weeks old at the beginning of the experimental timeline. All procedures were approved by the St. Vincent's Hospital Animal Research & Ethics Committee (AEC 031/21) in accordance with the National Institutes of Health Guidelines for the Care and Use of Laboratory Animals and conformed to the Code of Practice of the National Health and Medical Research Council of Australia.

2.2. Viral vectors

The control vector, AAV2.7m8 with a CMV-driven enhanced green fluorescent protein (AAV2.7m8-GFP; 2.44×10^{13} GC/mL), and regeneration "Regen" vector AAV2.7m8 with a CMV-driven hAtoh1 (tagged with 3xFLAG), hPou4f3 and *shKdm1a* (AAV2.7m8-Regen; 1.74×10^{13} GC/mL) were used (VectorBuilder; Supplementary Fig. 1A and B). Viral aliquots were stored at −80 °C and thawed before use. The viruses were formulated in phosphate buffered saline (PBS; pH7.4) supplemented with 200 mM NaCl and 0.001 % (w/V) pluronic F-68. The viral titres were confirmed by qRT-PCR and purity determined by SDS-PAGE followed by silver staining. HEK cells were used to validate expression of Atoh1 and Pou4f3 using immunostaining and qRT-PCR (Supplementary Fig. 1C and D). The shKdm1a sequence was based on published data in

which a reduction of Kdm1a is observed in HeLa cells (Wu et al., 2017; Zhang et al., 2016).

2.3. Auditory brainstem responses

The hearing thresholds of the mice were first established by measuring the auditory brainstem responses (ABRs) to tone pips 7 days prior to deafening. The thresholds were then re-measured 7 days after deafening, and 42 or 56 days after treatment (Fig. 1). For ABR threshold measurement, the mice were anaesthetized with ketamine (100 mg/kg) and xylazine (10 mg/kg). Needle electrodes were inserted at the vertex, pinna, and tail (grounding electrode). ABRs were evoked in each animal using 5 ms tone pips at seven log-spaced frequencies (half-octave steps from 5.6 to 45.2 kHz). The response was amplified, filtered, and averaged in a Lab-VIEW-driven data acquisition system. Sound level was raised in 5 dB steps from ≥10 dB below threshold to < 100 dB sound pressure level (SPL). ABR thresholds were defined as the lowest SPL level at which any wave could be detected, usually corresponding to the level step just below that at which the peak-to-peak response amplitude rose significantly above the noise floor (approximately 0.25 mV). When no response was observed at the highest sound level available, the threshold was designated as 100 dB SPL. The deafening criterion used was a confirmation of >85 dB SPL ABR hearing thresholds at the time of treatment.

2.4. Deafening

At day 0, mice received one intramuscular injection of DT at 10 ng/g or 20 ng/g (Table 1). For every experiment, 1–2 wild type mice from the same litter were also injected with DT as controls to confirm that the toxin itself was not causing hair cell or hearing function loss. A subset of mice were used to determine the optimal period of deafness prior to injection of the gene therapy. Mice were examined at 1, 2, and 3 weeks post-deafening to assess hearing threshold shifts and cochlear histology used to quantify hair cell and supporting cell densities. From these mice it was determined that gene therapy would be given at 2 weeks post-DT injection as the organ of Corti was damaged, but not completely flattened at this timepoint, with supporting cells remaining intact (Fig. 1).

2.5. Surgical delivery of gene therapy

Fourteen days post-DT treatment, the mice were injected with the Regen or control virus. A borosilicate glass micropipette (1.0 mm outer diameter × 0.78 mm inner diameter, Harvard Apparatus) was pulled with a micropipette puller (P-2000, Sutter) and then beveled to a final OD of ~30 μm, 30° angle tip with a micropipette beveller (BV-10, Sutter). The microneedle was mounted on a 10 μL gastight syringe (Hamilton) and the AAV viral vectors were loaded with 0.05 % (V/V) fast green dye (Sigma-Aldrich, St. Louis, MO) to aid visualisation during injection.

Table 1
Summary table of experimental animal cohort.

Deafening regime	Gene therapy	Treatment duration	N=
Pou4f3-DTR – mild deafening (Low DT dose −10 ng/g, 2 μL)	AAV2.7m8-GFP control	4 weeks	4
	AAV2.7m8-Regen	4 weeks	6
Pou4f3-DTR – severe deafening (High DT dose - 20 ng/g, 2 μL)	AAV2.7m8-Regen	6 weeks	3

Mice were anaesthetized using isoflurane (induced with 2–3 % isoflurane/oxygen in an induction chamber and 1 – 2 %, 1–1.5 L/min for maintenance, supplied to the animal via a face mask). Body temperature was maintained with a temperature-controlled heating pad during the surgical procedure. The left post-auricular region was shaved and cleaned with povidone-iodine 10 % solution (Betadine, Mundipharma, NZ). A drop of 1 % lignocaine hydrochloride (Sigma-Aldrich) was injected behind the left ear. Surgery was performed under aseptic conditions using an operating microscope (Zeiss OPMI 6, Carl Zeiss).

A post-auricular incision was made to expose the facial nerve and the sternocleidomastoid muscle. The facial nerve was dissected and moved dorsally to reveal the cochlea bulla underneath. The sternocleidomastoid muscle was detached from the temporal bone and retracted caudally to show the posterior semi-circular canal (PSCC) and the lateral semi-circular canal. Using a 0.6 mm diameter diamond burr (006 Kaisers, LifeHealthcare, WA), a hole was gently drilled in the PSCC. The perilymph leakage was continuously drained with absorbent paper points (DiaDent, Diamond Dental Industrial, Korea). The prepared microneedle was positioned near the PSCC using a three-axis micromanipulator (M-3333, Narishige, Japan). The tip was inserted through the hole and sealed with a drop of superglue. Two microliters of control or Regen virus (Table 1) was injected at 300 nL/min using a microinjection system (UltraMicroPump III with Micro4 Controller, World Precision Instruments, FL). After retracting the microneedle, the hole in the PSCC was sealed with a drop of superglue.

2.6. Histology

For collection of cochleae, the mice were sacrificed, and the temporal bones collected. The temporal bones were immersed in 4 % paraformaldehyde at room temperature for 2 h They were then washed in PBS and transferred into 0.12 M ethylenediaminetetraacetic acid (pH 7.4) for decalcification for up to 2 days at 4 °C. Cochlear wholemounts

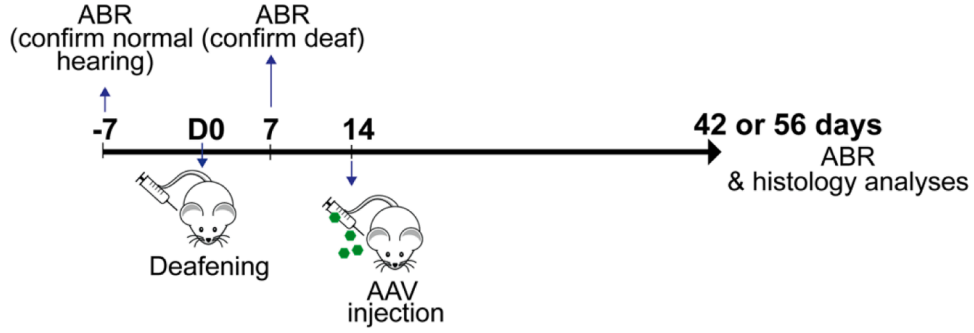

Fig. 1. Experimental timeline. A schematic diagram that depicts the experimental procedure. Seven days prior to deafening, a hearing test (ABR) was performed on adult Pou4f3-DTR mice (C57BL/6 J background; 4–6 weeks old) to confirm normal hearing. At D0, mice were deafened by injecting 10 ng/g or 20 ng/g of DT to eliminate hair cells. DT-induced threshold shifts were measured by a second ABR at D7. At D14, AAV carrying the multi-factor gene therapy (hAtoh1-FLAG, hPou4f3, shKdm1a) or control (GFP) was delivered into the cochlea via a posterior semi-circular canal injection. A final ABR was performed to assess hearing thresholds after treatment. At 4 or 6 weeks post-AAV treatment, the animals were terminated for histological analyses.

were prepared using fine-microdissection techniques. The wholemounts were then blocked in 0.2 % Tween-20 (P9416, Sigma-Aldrich) and 10 % heat inactivated donkey serum (D9663, Sigma-Aldrich) in PBS for 1 h The primary antibodies (Myo7a- 1:200 Proteus (Sapphire) Bioscience 25–6790, FLAG- 1:200 Sigma-Aldrich F3165, and Sox2- 1:100 R&D System AF2018-SP) were diluted in blocking solution and applied overnight at 4 °C. The relevant secondary antibodies (Alexa Fluor™ 488, 568 and 647 conjugated; Thermo Fisher Scientific) were diluted at 1:500 in blocking solution. The wholemounts were washed in blocking solution (3 × 5 min) and then transferred to secondary solution for 3 h at room temperature. To visualize the cochlear sensory epithelium structure, Alexa Fluor™ Plus phalloidin-405 (1:500, A30104, Thermo Fisher Scientific) was also added in the secondary antibody mix. The wholemounts were then washed and mounted in Pro-long gold anti fading reagent containing DAPI for nuclei visualization. The wholemounts were visualized and imaged using confocal microscopy (Nikon).

2.7. Confocal microscopy

Confocal microscopy was performed using a Leica TCS SP8 with Leica Application Suite Advanced Fluorescence (LAS AF) software V2.6.0. Sequential scanning with different laser channels was used for image acquisitions. Identical parameters (63x water immersion lens – NA 1.2, 1024 × 1024 with pinhole = 0.8 AU generating 16-bit images at 150 nm/pixel) were used to image all the samples. Optimal Z step size was determined by the Leica software and was calculated based on lens numerical aperture and immersion oil reflective index. The confocal images were processed using ImageJ software (www:\\imagej.nih.gov \ij) and Imaris 9.5.1. ImageJ maximum-projection Z-stack images were used for hair cell analysis and unprojected copies were imported to Imaris in *ims* format for supporting cell analysis.

2.8. Data analysis

The hair cell and supporting cell numbers were analysed at five cochlear frequencies (4, 5.66, 8, 16 and 32 kHz). These cells were quantified along the entire length of the basilar membrane. The length of the basilar membrane was measured, and the density of hair cells was calculated per mm of basilar membrane. Imaris 9.5.1 was used to evaluate co-localisation of different fluorescent markers in 'section' mode with view depth adjusted in 'extended' view. To count the supporting cells, a 3 × 3 × 3 median filter was applied. A spot detection method was then used with an estimated diameter of 6.5 μm applied for background subtraction. The supporting cell $Sox2^+$ nuclei were detected and quantified. Statistical analyses were performed where appropriate (sample $n \geq 3$). Normality was confirmed using the Shapiro–Wilk test and acceptance of statistical significance was set at a P-value of 0.05. Hair cell and supporting cell numbers were compared between GFP control and Regen treated cochleae at each frequency location via *t*-tests with correction for multiple comparisons. Comparison of site of transduction in GFP treated animals was via by a paired *t*-test. Functional assessment of hearing was by two-way ANOVA (treatment x frequency) with Tukey's multiple comparison test.

3. Results

3.1. Adult Pou4f3-DTR mouse deafening regime

We chose to use the Pou4f3-DTR deafness model for reliable and controllable hair cell loss (Tong et al., 2015; Golub et al., 2012). It was also important to choose a method that maintains the supporting cell population, since complete ablation of hair cells and supporting cells in the auditory sensory epithelium precludes rescue by Atoh1 overexpression (Izumikawa et al., 2008). We first conducted a study to confirm that the Pou4f3-DTR model selectively ablated hair cells and to identify the optimal DT concentration and timing of treatment.

Here, a subset of animals was tested for hair cell survival and hearing function at one-week, two-weeks, and three-weeks post DT (10 ng/g or 20 ng/g) treatment ($n = 12$; 2 animals per group/timepoint and dose). There was rapid hair cell degeneration resulting from the high dose of DT (20 ng/g), with almost complete loss of inner hair cells (IHCs) and outer hair cells (OHCs) after one week and complete loss two or three weeks post deafening. In comparison, the lower DT concentration resulted in near complete IHC loss and partial OHC loss after two weeks (Fig. 2A). At both DT doses, elevated hearing thresholds were observed after one week at ≥ 100 dB SPL thresholds across all the frequencies analysed (10 ng/g shown in Fig. 2B), whereas no shift in hearing thresholds was observed in the wild type-DT treated control mice. IHC loss occurred faster compared to the OHCs (Fig. 2C and D), reflective of the higher Pou4f3 expression in the IHCs versus OHCs (Tong et al., 2015). Of note, OHC loss was more rapid in the low frequency region compared to the higher frequencies at both DT concentrations (Fig. 2C and D). There was no loss of supporting cells 2 weeks after deafening, making the Pou4f3-DTR mouse a good model to evaluate hair cell regeneration therapies.

3.2. Viral delivery approach

We initially tested two methods for gene delivery into the cochleae of normal hearing mice- injection into the posterior semi-circular canal (PSCC; $n = 5$) or injection into the basal scala tympani (via the round window membrane) with PSCC fenestration to facilitate gene delivery throughout the cochlea ($n = 6$). Both approaches are standard methods used for viral delivery into the mouse cochlea. No significant shifts in hearing thresholds were observed with either approach when tested approximately 3 weeks post-test virus injection (Supplementary Fig. 2). All animals had stable or increased weights post-surgery indicating steady recovery. A slight head tilt post-surgery was observed, possibly caused by the positioning of the animal during the surgery and/or disturbance of fluids in the PSCC. With the PSCC approach, by 4 days post-surgery, the head tilt had resolved, whereas for the RW-PSCC approach the head tilt resolved at 6 days post-surgery. We did not observe any permanent signs of vestibular dysfunction in any of the AAV-treated animals, such as circling behaviour post-surgery. As the PSCC approach is anatomically easy and quick to identify in the mouse, and requires limited manipulation of the temporal bone, we selected this surgical route for subsequent experiments.

3.3. Quantification of hair cells and supporting cells after control and Regen gene therapy

We selected the AAV2.7m8 serotype for this study based on previous evidence of efficient supporting cell transduction, particularly the Lgr5+ supporting cells in the normal hearing adult mouse cochlea (Isgrig et al., 2019). Two weeks post-deafening with the low dose of DT (10 ng/g), adult mice were treated with the multi-factor gene therapy (AAV2.7m8-Regen; $n = 6$) or the control vector (AAV2.7m8-GFP; $n = 4$), which were unilaterally injected into the left cochlea via the PSCC approach. Approximately 28 days after the treatment, the cochleae were harvested, and the overall number of $Myo7a^+$ cells within the IHC and OHC regions were quantified and expressed as a density of cells per mm of basilar membrane. Here, it needs to be noted that we observed expression of both the Regen and GFP vectors in the contralateral (non-injected) cochleae, likely due to contralateral movement of the virus via the contiguous fluid pathways. As such, we could not use the contralateral cochleae as non-AAV-treated controls but instead used the GFP vector-treated cochleae as controls to compare to the Regen vector-treated cochleae for the remainder of the analyses.

There were very few $Myo7a^+$ IHCs in either the GFP controls or Regen-treated cochleae (Supplementary Fig. 3) and there was considerable variability across samples in the number of $Myo7a^+$ cells in the OHC region in both the GFP control and Regen-treated cochleae

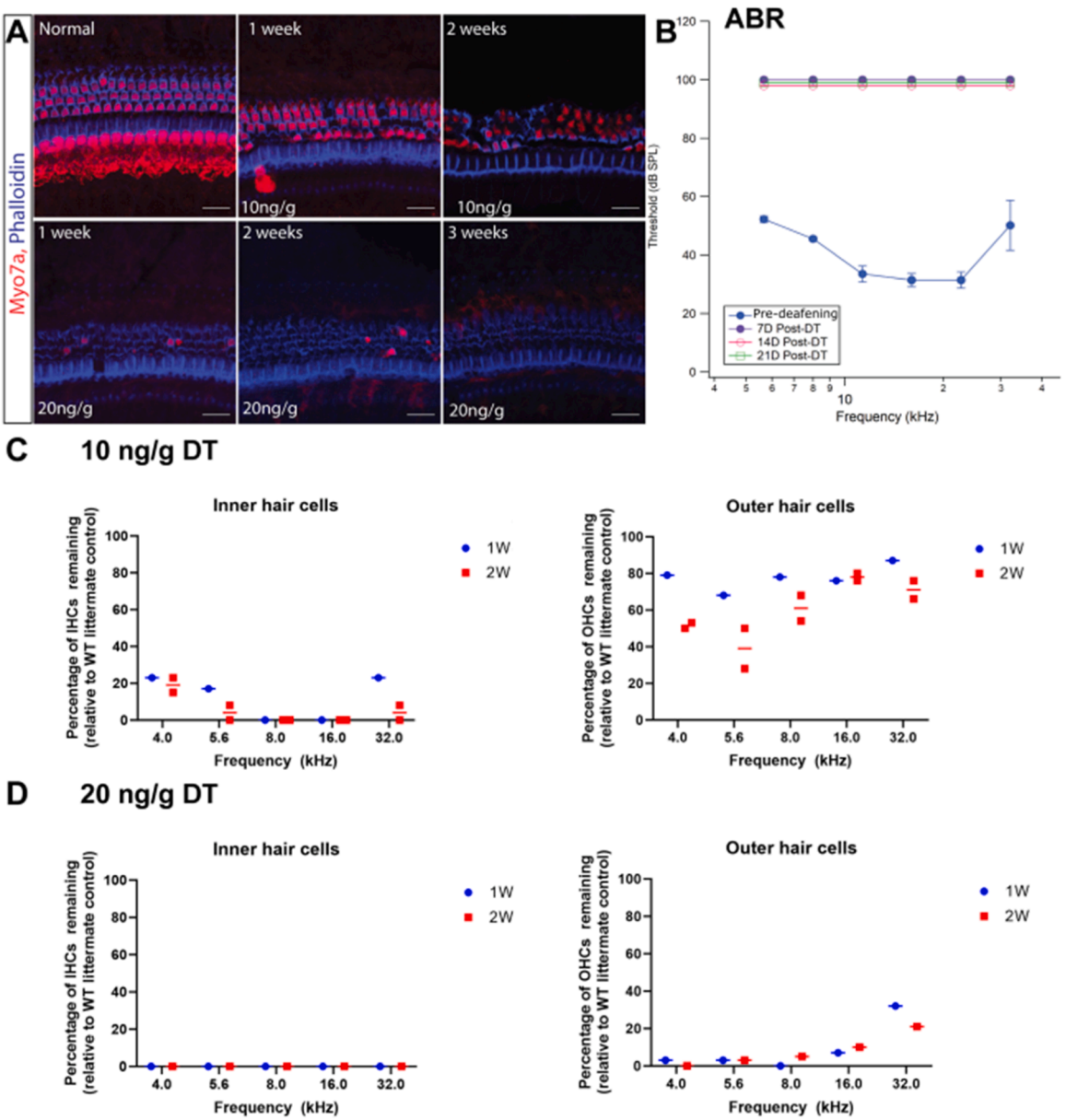

Fig. 2. Deafening regime in adult Pou4f3-DTR mice – comparison of 10 and 20 ng/g DT. (A) 63x images of cochlear sections at the 16 kHz apical-mid region from normal hearing and deaf mice at 1, 2- and 3-weeks post-DT injection using 10 ng/g DT or 20 ng/g DT, as indicated. Myo7a expression (a marker for hair cells) is shown in red, and phalloidin (a marker for F-actin to view cochlear structure) is shown in blue. Scale bar represents 25μm. (B) ABRs at pre-deafening ($n = 6$) and at 1-, 2- and 3-week post-deafening time points in mice receiving 10 ng/g DT ($n = 2$ per timepoint). (C) Quantification of remaining IHCs and OHCs at 1- and 2-weeks post-deafening in mice receiving 10 ng/g DT, and (D) in mice receiving 20 ng/g DT. Each symbol represents the percentage of hair cells remaining for an individual animal. In each animal, hair cells were quantified at five different locations along the cochlea. Results are presented as individual cochlear data point and mean for each timepoint and dose.

(Supplementary Fig. 3). The average OHC densities for the control cochleae at 8, 16 and 32 kHz were 106 ± 47, 100.8 ± 51.4 and 135.7 ± 70.1, respectively. The average OHC densities of the Regen-treated cochleae at 8, 16 and 32 kHz were 132.5 ± 58.3, 146.7 ± 65.7 and 104.3 ± 63.6, respectively. The densities of OHCs at the different frequencies were not statistically different between the GFP control and Regen treated mice. The supporting cell numbers ($Sox2^+$ cells) at 4 weeks post-treatment was next compared between the two groups. We examined the supporting cells within the inner and outer regions of the cochlear sensory epithelium. While there was some variability in supporting cell numbers, no statistically significant difference in $Sox2^+$ cells was observed across the frequencies analysed and between the control and treatment groups (Supplementary Fig. 4).

(i) Characterisation of GFP expression in residual hair cells and supporting cells after control gene therapy

Hair cell and supporting cell transduction efficiency was assessed by quantifying the percentage of remaining hair cells (identified by anti-Myo7a antibody) and supporting cells (identified by anti-Sox2 antibody) with GFP expression across five frequency regions from apex to base. Analysis of the cochlea 4 weeks after gene delivery showed GFP expression in remaining IHCs, OHCs and supporting cells in mice that were injected with AAV2.7m8-GFP ($n = 4$; Fig. 3). Of the animals that had some remaining IHCs ($n = 2$), the transduction efficiency across the 5 frequency regions analysed was ~42.5 % (average density of 2 GFP^+/$Myo7a^+$ IHCs/mm of basilar membrane). For the remaining OHCs, the transduction efficiency was 33 ± 14.7 % (mean ± standard error; $n = 3$;

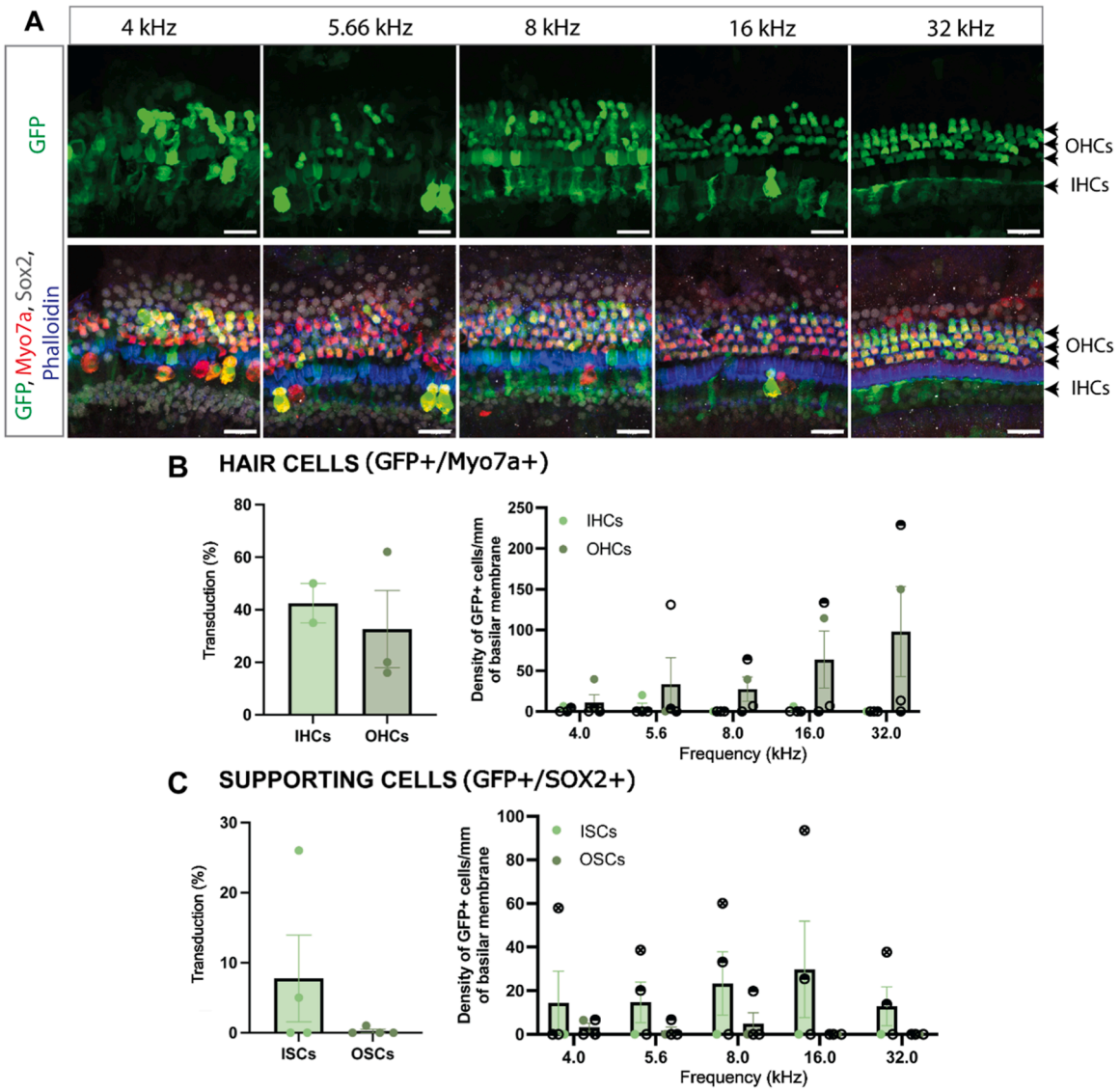

Fig. 3. Transduction efficiency of the deaf cochlea with AAV2.7m8-GFP. (A) Unilateral injection ($n = 4$) of AAV2.7m8-GFP into adult mouse inner ear via the PSCC approach led to the IHCs, OHCs and some inner and outer supporting cells being transduced throughout the entire cochlea. GFP expression is shown in green, Myo7a expression (a marker for hair cells) is shown in red, phalloidin (a marker for F-actin to view cochlear structure) is shown in blue and Sox2 expression (a marker for supporting cell nuclei) is shown in grey. 63x images of the cochlea at 5 regions are shown. Scale bar represents 25 μm. (B) Quantification of IHC ($n = 2$) and OHC ($n = 3$) transduction efficiency and density of GFP expressing hair cells ($n = 4$ mice) at five frequency locations (paired multiple *t*-tests with correction: no statistically significant difference observed in 4–32 kHz, $p > 0.05$). (C) Quantification of inner supporting cells (ISCs) and outer supporting cells (OSCs) transduction efficiency ($p = 0.3155$) and density of GFP expressing supporting cells ($n = 4$ mice) at five frequency locations (paired multiple *t*-tests with correction: no statistically significant difference observed in 4–32 kHz, $p > 0.05$). Each circle represents the average infection efficiency of each animal. For each animal, hair cell transduction was quantified at five different locations along the cochlea. Error bars represent standard error of mean.

average density of 47 $GFP^+/Myo7a^+$ OHCs/mm of basilar membrane).

Cochlear supporting cells contain different cell types: Hensen's cells, Deiters cells, inner/outer pillar cells, inner phalangeal cells, and inner border cells. As these cells are the target population for hair cell regeneration therapies, their transduction efficiency in the deaf cochlea is a critical factor. We observed low transduction of the inner cochlear supporting cells, including inner pillar cells and inner phalangeal cells. The average transduction efficiencies of the inner supporting cells at the five frequency locations analysed was 8 ± 1.7 % ($n = 4$). There was also limited supporting cell transduction in the outer sensory region, with only <1 % of the outer supporting cells being transduced in the apical-mid region. No statistically significant difference was detected between the transduction efficiencies of both types of supporting cells ($p > 0.05$, paired *t*-test), but the low transduction efficiency made this test underpowered.

(ii) Characterisation of hAtoh1 expressing hair cell-like cells after Regen gene therapy

The Regen vector used was designed to tag cells expressing hAtoh1 with a FLAG marker. The $FLAG^+$ cells were categorised into three definitions: **(1)** Mature hair cells ($FLAG^+/Myo7a^+$ cells), **(2)** transitioning hair cell-like cells ($FLAG^+/Sox2^+$), and **(3)** non-sensory immature hair cells ($FLAG^+/Myo7a^-/Sox2^-$). Here, we note that $FLAG^+/Myo7a^+$ cells may also represent residual hair cells that have been transduced with the virus.

3.3.1. Mature hair cells ($FLAG^+/Myo7a^+$ cells)

Upon examination of the Regen-treated cochleae 6 weeks post-deafening and 4 weeks post-treatment, there were numerous $FLAG^+/Myo7a^+$ cells from the apex to mid cochlear turns, predominantly in the

OHC region and a few in the IHC region in 5 of the 6 animals tested (Fig. 4A–D). FLAG$^+$/Myo7a$^+$ cells were not detected in the basal region of the cochlea (~32 kHz). The average density of FLAG$^+$/Myo7a$^+$ cells in the OHC region at each of the frequencies analysed was ~27 ± 19 cells/mm of basilar membrane (Fig. 4E). Of note, in individual animals with low numbers of inner supporting cells at the 5.66 and 16 kHz region (See Supplementary Fig. 4A), there was a corresponding higher number of FLAG$^+$/Myo7a$^+$ cells, which could implicate the transdifferentiation of supporting cells into hair cells (Fig. 4E). However, the overall density of FLAG$^+$/Myo$^+$ cells in the Regen animals were not different to the GFP$^+$/Myo$^+$ cell density in the control vector animals (Table 2).

The FLAG$^+$/Myo7a$^+$ cells had differing morphologies with some displaying the typical pear-shaped inner hair cell-like morphology and others with a more spherical morphology (Fig. 4A; white arrows). There were some ectopic FLAG$^+$/Myo7a$^+$ cells within the OHC region, however, given the disorganisation of the sensory epithelium that occurs after deafening, it was difficult to interpret if the ectopic cells were new hair cell-like cells or remaining hair cells that had been transduced with the virus.

3.3.2. Transitioning hair cell-like cells (FLAG$^+$/Sox2$^+$)

FLAG$^+$/Sox2$^+$cells were present in 3 out of the 6 animals analysed, indicating the presence of cells transitioning from a supporting cell to a hair cell-like lineage. Interestingly, these cells were predominantly observed in the base (16–32 kHz, at an average density of 18 ± 38 cells/mm of basilar membrane) and were predominantly outer or inner pillar cells (Fig. 4D; orange arrows).

3.3.3. Non-sensory immature hair cells (FLAG$^+$/Myo7a$^-$/Sox2$^-$)

A sub-population of FLAG$^+$ cells did not co-localise with Myo7a or Sox2 (FLAG$^+$/Myo7a$^-$/Sox2$^-$) cells (Fig. 4B; blue arrows). Consistent with the pattern of normal hair cell development, we hypothesise that these may be immature hair cells, whereby the supporting cells have downregulated their expression of Sox2 and upregulated Atoh1, as they transition into a hair cell-like lineage. Most of these cells were identified in the apical to mid regions of the cochlea. On average there was a density of ~10 ± 8 FLAG$^+$/Myo7a$^-$/Sox2$^-$ cells/mm of basilar membrane at the 4–16 kHz frequencies analysed.

3.3.4. Myo7a$^+$/Sox2$^+$ cells

We observed cells with weak expression of Myo7a$^+$ in the deaf organ of Corti that also displayed Sox2 signal (Myo7a$^+$/Sox2$^+$; Fig. 5). The cells had a spindle-like morphology and were mostly detected above the third row of the OHCs, colocalising with the third Deiters supporting cells (Fig. 5A). These cells showed antibody staining for Sox2 in their nuclei, consistent with immature hair cells. This pattern of expression was observed in both the GFP control and Regen-treated cochleae. However, the density of cells across the five frequencies analysed was statistically significantly higher in the Regen-treated cochleae, compared to the control (Fig. 5B; $n = 5$; unpaired t-test, $p < 0.05$*). Interestingly, a trend of increasing Myo7a$^+$/Sox2$^+$ cells were detected in the more severely damaged cochleae, as measured by the overall loss of hair cells. A non-linear regression exponential growth curve was fitted to the density of Myo7a$^+$/Sox2$^+$cells relative to density of Myo7a$^+$ cells in the Regen-treated cochleae. There was a significant interaction between increased Myo7a$^+$/Sox2$^+$cells and reduced Myo7a$^+$ OHCs (Fig. 5C, R^2=0.33, Pearson correlation analysis, $p < 0.001$***).

3.4. Presence of hAtoh1-FLAG expressing cells after severe deafening

To evaluate if regeneration could be achieved after severe deafening, we next injected the Pou4f3-DTR mice with the high dose of DT (20 ng/g; $n = 3$). The multi-factor gene therapy vector (AAV2.7m8-Regen) was injected into the cochlea of adult mice 2 weeks post-deafening. Approximately 42 days after the gene therapy treatment, the cochleae were harvested, and the overall number of IHCs and OHCs quantified (Myo7a$^+$ cells) and expressed as a density of cells across 1 mm of the basilar membrane.

With the 20 ng/g DT dose, there was significant degeneration of the sensory epithelia, as evidenced from the phalloidin staining (Fig. 6A). Nevertheless, after treatment with the Regen vector, we observed in 2 of the 3 animals tested that there were some remaining (or regenerated) OHCs after >8 weeks post-deafening (Fig. 6B and C). We attempted to quantify the Sox2$^+$ cells, but the signal was extremely weak, and it was difficult to determine if the Sox2 was downregulated and/or the supporting cells were dying. hAtoh1-FLAG expressing cells were present in the cochleae of all three severely deafened animals, but only one animal showed FLAG$^+$/Myo7a$^+$ cells (at a density of ~6 cells/mm of basilar membrane in the 8 kHz region). There were several FLAG$^+$ non-sensory cells at some of the frequencies analysed (5.66, 16, 32 kHz), with an average density of ~7 ± 4 cells/mm of basilar membrane (Fig. 6D).

3.5. Functional assessment

To test the functional effect resulting from the increase in hAtoh1-FLAG$^+$ cells after our multi-factor gene therapy in the partially and severely deaf cochlea, ABR thresholds were measured seven days prior to deafening, seven days post deafening, and four- or six-weeks post gene therapy treatment (Supplementary Fig. 5). ABRs measured seven days after deafening indicated that all the animals were severely deaf across all frequencies measured, (Two-way ANOVA with Tukey's Multiple comparison test, $p < 0.001$). When thresholds were re-measured post gene therapy treatment, there was no statistically significant improvement in hearing thresholds after treatment. However, we did observe an improvement in hearing threshold (10–25 dB threshold shift) in the 5.66–11.33 frequencies in 2 out of the 6 animals that were deafened and treated with AAV2.7m8-Regen.

4. Discussion

There is a significant need for the development of an effective approach to regenerate hair cells as a treatment for hearing loss. In the immature cochlea, Atoh1 is the first transcription factor to be upregulated in differentiating hair cell progenitors. Overexpression of Atoh1 or manipulation of cell signalling pathways including the Notch or Wnt pathways to activate Atoh1 leads to generation of new hair cell-like cells in non-sensory regions of the embryonic or neonatal mouse cochlea (Liu et al., 2012; Kelly et al., 2012; Bramhall et al., 2014; Mizutari et al., 2013). However, this regenerative ability rapidly declines in the first post-natal week, with limited efficiency in adults (Liu et al., 2012). Changes to the epigenetic landscape of the cochlea has been correlated with the loss in regenerative capacity of the adult cochlea (Iyer et al., 2022). Significant efforts to augment the reprogramming activity of the mature cochlea by manipulating multiple signalling pathways or combinations of other hair cell transcription factors have been tested (Costa et al., 2015; Walters et al., 2017; Chen et al., 2021; Lee et al., 2020), but the efficacy of these approaches were primarily tested in vitro or in normal hearing adult mice. Here, we tested if overexpression of Atoh1 and Pou4f3, along with inhibition of Lsd1, would improve the efficiency of hair cell reprogramming in the deaf adult mouse cochlea. We observed no significant difference in hair cell density post-treatment, compared to the GFP vector-treated controls. However, in the Regen-treated cochlea, several new Atoh1$^+$ hair cell-like cells were detected in both the partially and severely deafened cochlea. Given previous evidence that the severely deaf cochlea is unresponsive to Atoh1 overexpression (Izumikawa et al., 2008), the detection of any Atoh1 expressing cells 6 weeks after our multi-factor gene therapy is notable.

There were several factors that required consideration in the design of this study. Firstly, an adult deafness model that could reliably eliminate hair cells, whilst maintaining the supporting cell population was required. We selected the Pou4f3-DTR model as, compared to the other

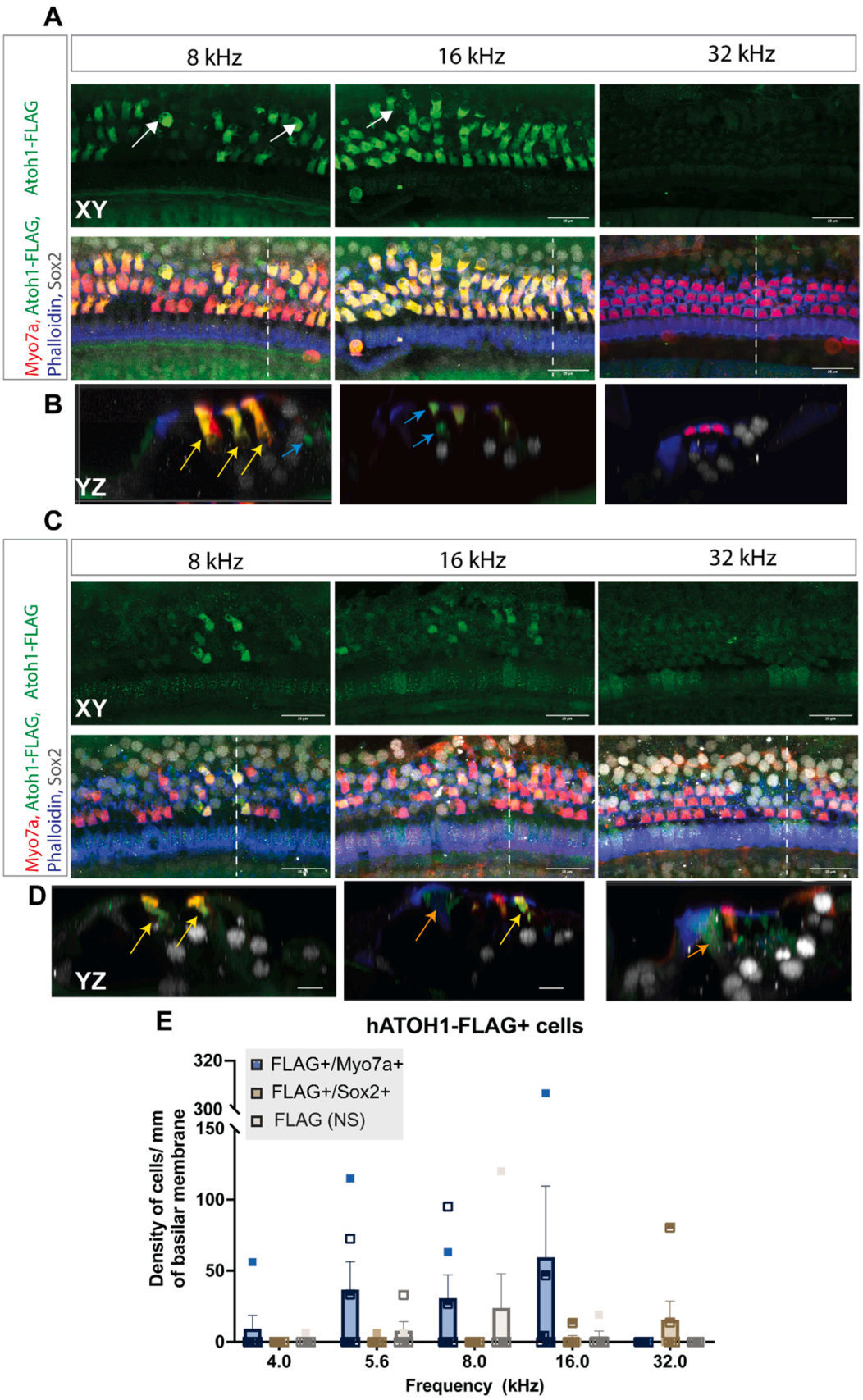

(caption on next page)

Fig. 4. hAtoh1-FLAG expressing cells in the Regen-treated cochlea. (A-D) 63x images of two representative cochleae at 3 frequency regions where hAtoh1-FLAG expression is shown in green, Myo7a expression (a marker for hair cells) is shown in red, phalloidin (a marker for F-actin to view cochlear structure) is shown in blue and Sox2 expression (a marker for supporting cell nuclei) is shown in grey. (A) XY-plane images of Animal 1 at 8, 16 and 32 kHz. White arrows show the ectopic hair cells. (B) Cross-section (YZ-plane) image at region depicted with dashed line in A. Yellow arrows show FLAG$^+$/Myo7a$^+$ cells. Blue arrows show FLAG$^+$ non-sensory cells. (C) XY-plane images of Animal 2 at 8, 16 and 32 kHz (see also Supplementary Video 2). (D) Cross-section (YZ-plane) image at region depicted with dashed line in C. Yellow arrows show FLAG$^+$/Myo7a$^+$ cells and orange arrows show FLAG$^+$/Sox2$^+$ cells. Scale bar of XY images is 25μm and YZ is 10 μm. (E) Quantification of FLAG$^+$ cell density after treatment with the Regen vector ($n = 6$) at five different locations along the cochlea. Each point represents the FLAG$^+$ cells of each animal, and error bars represent standard error of mean. FLAG+(NS) represents non-sensory cells that express FLAG.

Table 2
Comparison of GFP$^+$ or FLAG$^+$ cell densities in control and Regen treated animals, respectively (combining inner and outer cell counts).

	Myo$^+$		Sox2$^+$	
Frequency (Hz)	GFP$^+$ (Control) (cells/mm)	FLAG$^+$ (Regen) (cells/mm)	GFP$^+$ (Control) (cells/mm)	FLAG$^+$ (Regen) (cells/mm)
4	13.9 ± 22.0	9.4 ± 22.9	17.8 ± 27.0	0.0 ± 0.0
5.6	38.7 ± 62.3	36.8 ± 47.9	16.3 ± 19.5	1.1 ± 2.6
8	27.6 ± 29.8	29.8 ± 39.2	28.3 ± 32.8	2.1 ± 5.2
16	65.4 ± 71.8	60.7 ± 125.0	29.8 ± 44.2	2.2 ± 5.5
32	98.1 ± 110.5	0.0 ± 0.0	12.9 ± 17.8	15.6 ± 32.1

available deafness models (noise exposure, antibiotics), the hair cell loss post-DT treatment is more consistent and can be modulated reliably with adjusted DT concentrations (Tong et al., 2015). Of key relevance to this study, it permits preserved supporting cells consistent with the pathology observed in human hearing loss (C. Kaur et al., 2023). Nevertheless, it should be considered that although the higher dose of DT (20 ng/g) effectively ablates hair cells, it may not reflect the natural progression of hearing loss in humans or other animal models. In particular, the DT causes IHCs to be lost more rapidly than OHCs, which contrasts with findings in humans and animals where OHCs are generally more vulnerable to damage and degeneration, particularly in the high frequency regions of the cochlea (C. Kaur et al., 2023; Raphael and Altschuler, 1991; Kujawa and Liberman, 2009). Furthermore, while the lower DT dose (10 ng/g) might be more physiologically relevant, the partial loss of hair cells, especially the OHCs, could affect the interpretation of regeneration strategies targeting both IHCs and OHCs. However, DT is an effective experimental tool to damage hair cells with high consistency and keep the organ of Corti structure intact to assess the feasibility of new hair cell formation. In future studies, additional, and more clinically relevant deafness models should be tested, such as noise-induced hearing loss, that more closely follow common cochlear pathologies. The PSCC delivery approach was selected due to the relative ease of accessing the injection site and the minimal impact on hearing thresholds post-treatment, consistent with other studies (Isgrig and Chien, 2018). Despite controlling for these factors, we still observed considerable variation in hair cell densities across both the control and treatment groups. Although we observed a trend of increased total hair cell numbers post-treatment (relative to control), statistically significant results could not be achieved due to the variability. Other factors that could influence outcomes relate to the AAV transduction such as promoter (CMV vs cell-specific promoter), serotype and titre, and toxicity that may occur from GFP overexpression (Eckrich et al., 2019; Verdoodt et al., 2021). Additionally, the mouse inner ear is extremely small and inevitably there can be complications from surgery, thus needing to treat

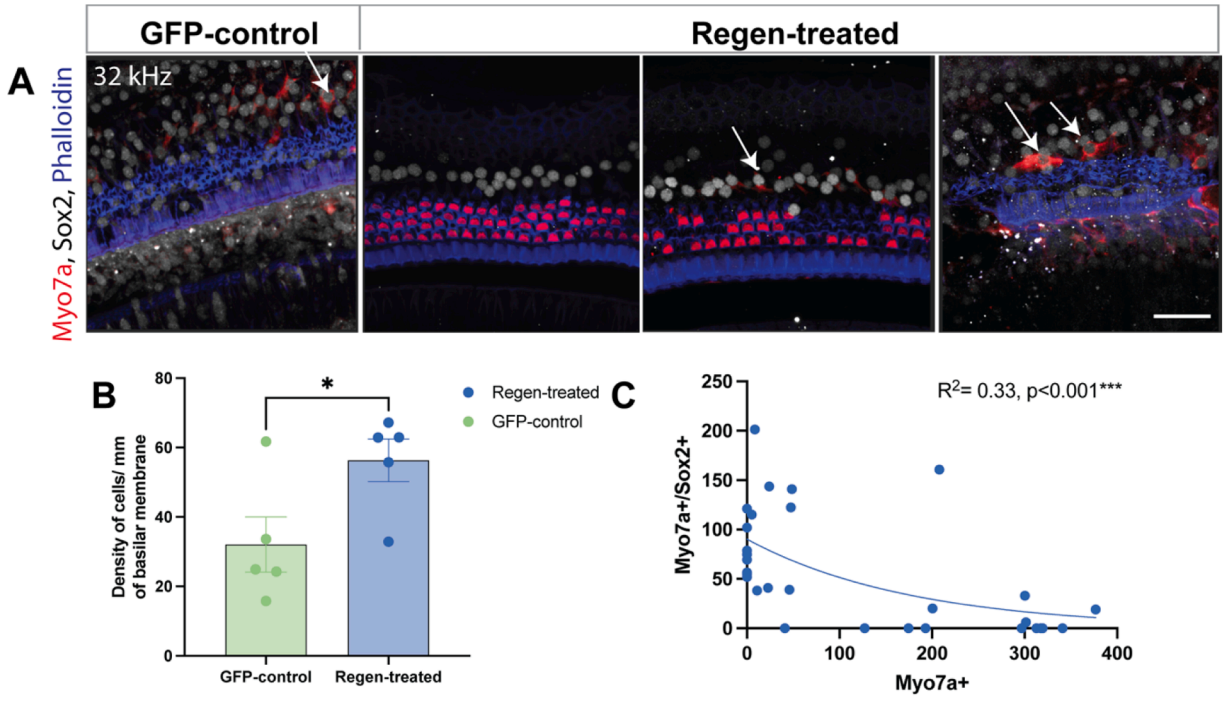

Fig. 5. Presence of Myo7a$^+$/Sox2$^+$ cells in both the GFP control and Regen-treated cochleae. (A) Representative 63x images of Myo7a$^+$/Sox2$^+$ cells in the cochlea in the basal region (32 kHz). Myo7a expression (a marker for hair cells) is shown in red, phalloidin (a marker for F-actin to view cochlear structure) is shown in blue and Sox2 expression (a marker for supporting cell nuclei) is shown in grey. White arrows show Myo7a$^+$/Sox2$^+$ cells. Scale bar is 30 μm. (see also Supplementary Video 1). (B) Quantification of Myo7a$^+$/Sox2$^+$ cells across five different locations along the cochlea in the GFP-control and Regen-treated cochleae ($n = 5$). Each point represents the average density of cells across the five frequencies tested ($p < 0.05$*, unpaired t-test). (C) Correlation between the density of Myo7a$^+$ OHCs and the number of Myo7a$^+$/Sox2$^+$ cells in the Regen-treated cochlea (Spearman correlation test, R^2=0.33, $p < 0.001$***). Error bars represent standard error of mean.

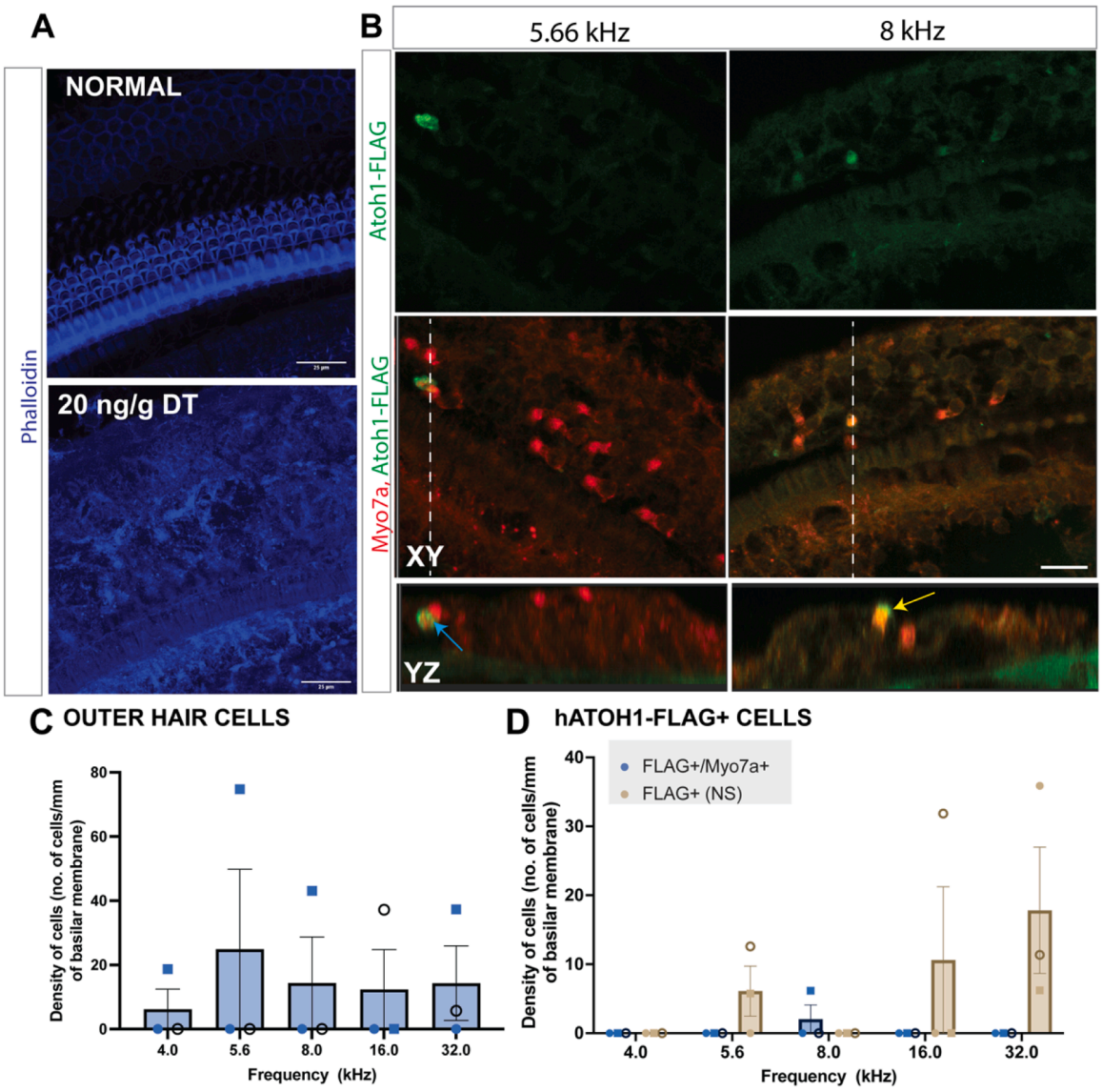

Fig. 6. FLAG-expressing cells in the severely deaf cochlea post-treatment with AAV2.7m8-Regen. (A) Phalloidin staining of normal cochlea at 32 kHz versus deafened cochlea (20 ng/g DT) showing significant disorganisation of the sensory epithelia 8 weeks post-deafening. (B) Histology analyses at week 6 post unilateral injection of AAV2.7m8-Regen into the severely deaf adult mouse inner ear via the PSCC approach. FLAG expression is shown in green (hAtoh1 expressing cells) and Myo7a expression (a marker for hair cells) is shown in red. 63x images of the cochlea at 2 regions of the cochlea are shown. Scale bar represents 30 μm of XY-plane images and 10 μm in the YZ plane. Blue arrow shows a $FLAG^{+}$ non-sensory cell. Yellow arrow shows a $FLAG^{+}/Myo7a^{+}$ cell. (C) Quantification of OHC density after treatment with AAV2.7m8-Regen ($n = 3$). (D) Quantification of $FLAG^{+}$ cell density after treatment with AAV2.7m8-Regen ($n = 3$). Each marker represents the hair cell number of an individual animal at five different locations along the cochlea. Error bars represent standard error of mean.

multiple animals to achieve reliable data. As such, transitioning to larger animal species warrants further exploration. Future experimental planning for the development of gene therapy approaches for hearing loss will require careful consideration of the above factors to mitigate variability.

Treatment of the deaf cochlea with our multi-factor gene therapy approach led to the generation of some new hair cell-like cells. Of note, animals with low numbers of inner supporting cells at the 5.66 and 16 kHz region had correspondingly higher number of $FLAG^{+/}Myo7a^{+}$ cells, implicating the transdifferentiation of supporting cells into hair cells. The transdifferentiation observed here is similar to the mechanism of hair cell regeneration in lower vertebrates (Warchol, 2011), whereby supporting cells behave as hair cell precursors under the influence of hair cell genes such as Atoh1 (Cafaro et al., 2007). In birds, supporting cells can also respond by entering the cell cycle, proliferating, and then transdifferentiating into hair cells. In this deaf adult mouse model, we hypothesise that the mechanism underlying the hair cell regeneration was through supporting cell priming via Lsd1 inhibition, and the subsequent transdifferentiation upon upregulation of genes including Atoh1 and Pou4f3. Notably, the overall supporting cell infection efficiency was only ~8 % with the GFP control vector in the deaf cochlea, and as such this is the maximal transdifferentiation that could be expected with the therapy. These findings highlight a key limitation: the AAV2.7m8-GFP vector may not be the optimal approach for specifically targeting supporting cells, which are essential for successful regeneration. The low transduction efficiency undermines the potential for effective hair cell regeneration, underscoring the need for improved vectors or alternative strategies to enhance gene delivery to supporting cells. Strategies focused on improving supporting cell transduction in the deaf cochlea, including testing novel AAV serotypes and/or targeted nanoparticles, could lead to improved efficacy of this therapy. Given that supporting cells play a critical role in hearing, it will be necessary to develop a

strategy that promotes proliferation of supporting cells prior to trans-differentation, as observed in birds, to restore hearing function. Indeed, there is now evidence in the neonatal mouse cochlea that activation of Sonic Hedgehog signalling can prompt cell cycle re-entry and the generation of new hair cells (Chen et al., 2017; Lu et al., 2013). Furthermore, manipulation of the ERBB2 pathway has also shown to activate supporting cell proliferation with increased hair cell numbers in neonatal mice (Zhang et al., 2018). Future studies will be to assess the functional maturation of regenerated hair cells, including their ability to form synapses with auditory neurons and restore auditory function. This will likely involve combining gene therapy with other approaches such as neurotrophic factor delivery or synaptic repair strategies.

In severe cases of deafness, where there is also supporting cell degeneration post-hair cell loss, the remaining cells become less responsive to Atoh1 (Izumikawa et al., 2008). A severely lesioned cochlea is defined as a "flat epithelium", as the basilar membrane becomes covered by a layer of flat or cuboidal simple epithelial cells. While the origin and heterogeneity of these cells remain unclear, prior studies have indicated that these non-sensory epithelial cells represent de-differentiated supporting cells and/or cells that have migrated to the sensory epithelium from flanking regions (Kim and Raphael, 2007). Moreover, it has been shown in a neomycin-deafened guinea pig cochlea that these epithelial cells undergo a robust proliferative response, evidenced by the downregulation of the cell cycle inhibitor $p27^{kip1}$ (Kim and Raphael, 2007). The deafness model used in this study allowed the supporting cells to remain intact. Following Regen treatment, we observed the presence of Atoh1 expressing cells in both the partial and severely deaf cochlea that co-localised with non-sensory epithelial cells. Although understanding the molecular mechanism of this approach and further optimisation of the therapy will be the focus of future experiments, these findings implicate the possibility that epithelial cells in a severely deaf cochlea can be manipulated to convert into new hair cell-like cells using a genetic and epigenetic reprogramming approach. In a related study using a combinatorial genetic approach in severely deafened guinea pigs, expression of Atoh1 along with Gfi1, Pou4f3, and Six1 enhanced the generation of myosin-positive cells in the flat epithelium, albeit under the basilar membrane, with an associated neural regeneration response (Liu et al., 2024). Given that most patients that receive a cochlear implant have severe hair cell loss (Nadol et al., 1994), an improved understanding of the biology of these non-sensory epithelial cells including their potential for gene therapy manipulation will be important for the development of hearing loss therapies in many

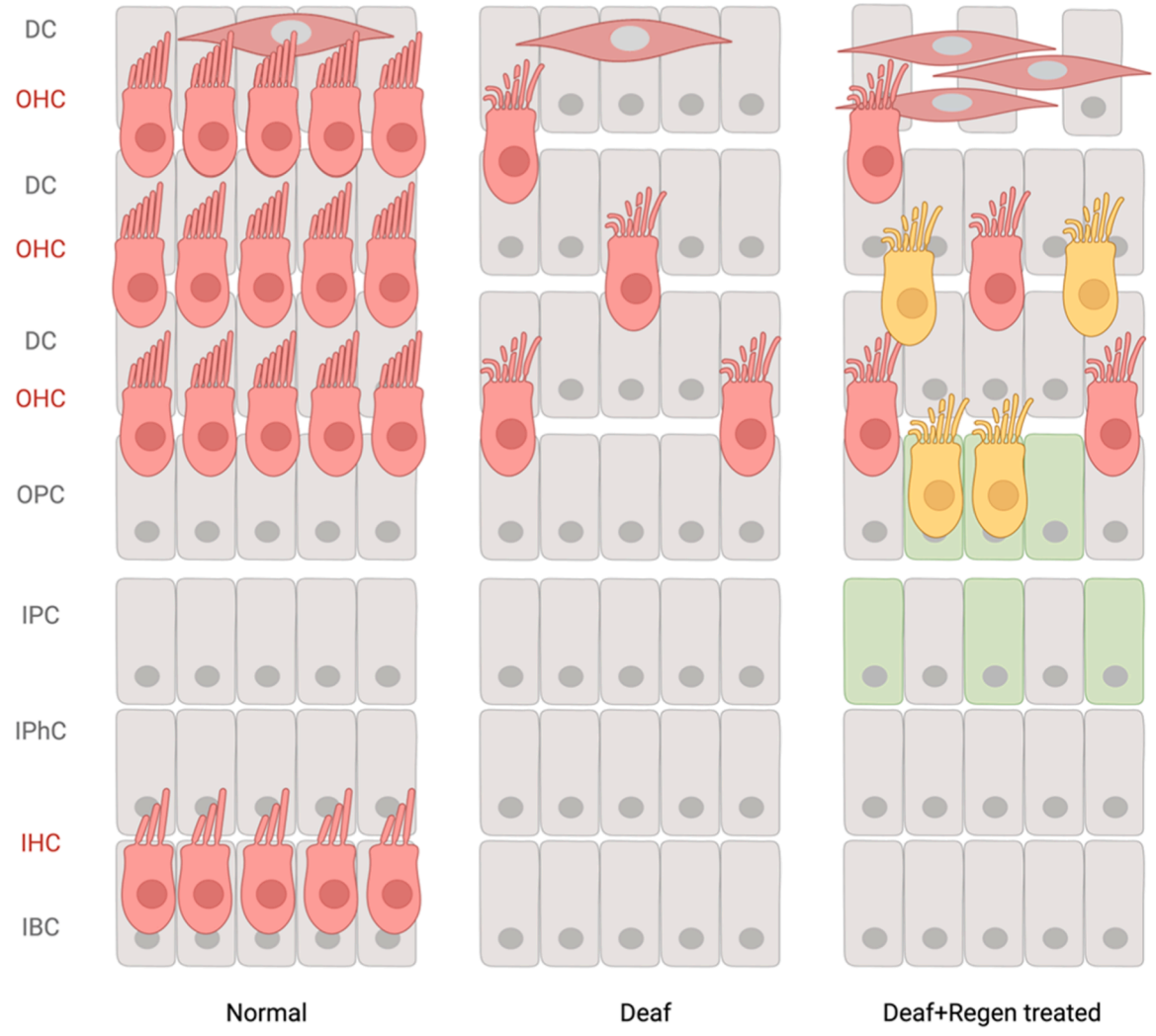

Fig. 7. Schematic showing the normal organ of Corti, the organ of Corti following DTR damage (10 ng/g; partial), and the organ of Corti following DTR damage and AAV2.7m8-Regen treatment. Cell types are labelled as follows: inner border cell (IBC), inner hair cell (IHC), inner phalangeal cell (IPhC), inner pillar cell (IPC), outer pillar cell (OPC), outer hair cell (OHC), and Deiters cell (DC). Supporting cells are indicated in gray ($Sox2^{+}$). Original hair cells are indicated as red cells ($Myo7a^{+}$). Following damage, the IHCs are lost, but a few OHCs remain. After Regen treatment, there are new hair cell-like cells ($FLAG^{+}/Myo7a^{+}$; yellow cells) and immature hair cells ($FLAG^{+}/Sox2^{+}$; green cells). Some spontaneous or treatment induced regenerated hair cells (red spindle cells with grey nuclei; $Myo7a^{+}/Sox2^{+}$) are detected in the third DC region. The non-sensory cells that express FLAG are not shown here. Image created with BioRender.com.

clinical cases.

Previous studies have reported that the neonatal cochlea possesses some spontaneous regenerative capacity after damage (Bramhall et al., 2014; Cox et al., 2014; McGovern et al., 2018; Hu et al., 2016). Increased number of spontaneous and regenerated hair cells can be achieved when the cochlea is treated with a pharmacological inhibitor of the Notch pathway (Bramhall et al., 2014; Mizutari et al., 2013). However, approximately 1 week after birth, this spontaneous regenerative potential diminishes significantly (Cox et al., 2014). This age-dependent decline has also been correlated with a limited capacity for the cochlea to respond to Atoh1 gene therapy (Liu et al., 2012; Kelly et al., 2012), which in turn has been recently correlated to epigenetic changes. The accumulation of chemical changes on DNA or histones causes hair cell loci to become epigenetically inaccessible as the morphology of the chromatin changes to a heterochromatin or gene repression state (Jen et al., 2019; Tao et al., 2021; Iyer et al., 2022). In our damage model, we observed some Myo7a^{+} cells that were also positive for Sox2 (Fig. 7). This pattern of expression, restricted to the third Deiter's cell region in the deaf cochlea, can also be found in normal (undamaged cochleae) and are similar to the spontaneously regenerated cells in the neonatal mouse cochlea (Bramhall et al., 2014; Cox et al., 2014). Interestingly, the Regen treated cochlea showed a higher number of Myo7a^{+}/Sox2^{+} cells (when compared to the GFP control) that correlated to the extent of deafening. Hair cell loss in the Pou4f3-DTR model occurs via an apoptotic mechanism (Ivanova et al., 2005), similar to that observed in noise or drug-induced hair cell death (Henderson et al., 2006; Gunewardene et al., 2013). As such, our observations have important clinical implications for hair cell regenerative therapies. However, it needs to be emphasised that any possible spontaneous regeneration detected here could be specific to this deafness model. For instance, it was shown in the neonatal cochlea that spontaneous regeneration occurred in a DTR model, but not in the neomycin-induced deafness model (Hu et al., 2016). This was attributed to differences in the level of Wnt activation, whereby they showed a threshold level of Wnt signalling was necessary for spontaneous regeneration to occur. Of note, Lsd1 is a regulator of the Wnt pathway in several systems (Chen et al., 2016; Zhou et al., 2016; Lei et al., 2015), and while it was not tested in this study, we postulate that *shKdm1a* (which inhibits Lsd1) may have contributed to our regeneration outcomes.

There are several barriers to the translation of hair cell regenerative therapies to the clinic. Firstly, there is a need to test the maturity of the newly regenerated hair cell-like cells in this study, including their capacity to form functional connections with the auditory neurons. To date, most of the reports have indicated that the new hair cell-like cells are immature. Secondly, conventional gene therapy approaches utilise constitutive gene expression. Persistent Atoh1 expression can lead to cell toxicity, thus there is a need for a system that supports temporal gene upregulation in the cochlea. In other systems including the brain and retina, significant headway has been made to control transgene expression using AAV in vivo. Potential approaches include the tetracycline-transcription inducible system (Georgievska et al., 2004; Dogbevia et al., 2016; Zeng et al., 2008; Mansuy et al., 1998) and/or drug-regulated destabilising domain systems (Datta et al., 2018; Iwamoto et al., 2010; Tai et al., 2012; Quintino et al., 2013; Quintino et al., 2018). Thirdly, approaches such as functionalised nanoparticles or cell-specific promoters to target only supporting cells may be required. An additional consideration is whether the supporting cell gene network needs to be completely suppressed prior to the activation of hair cell genes for effective regeneration. Finally, and importantly, the treatment needs to improve hearing function reliably and persistently. Here, we did not observe any significant improvement in hearing function, thus implicating that the newly regenerated hair cells may still be immature and not contribute to hearing at this stage.

Collectively, our findings suggest that a multi-factor gene therapy approach that targets the genome and epigenome can promote hair cell regeneration in the partial and severely deaf cochlea, the extent of which was limited by the efficiency of supporting cell transduction. To our knowledge, the presence of improved spontaneous regeneration that also correlates with the extent of deafening has yet to be reported in the treated adult cochlea.

Author statement

On behalf of all the authors, I can confirm that:

All authors should have made substantial contributions to all of the following:

1. The conception and design of the study, or acquisition of data, or analysis and interpretation of data.
2. Drafting the article or revising it critically for important intellectual content.
3. Final approval of the version to be submitted.

Ethical approvals

All procedures involving animals were approved by the St. Vincent's Hospital Animal Research & Ethics Committee (AEC 031/21) in accordance with the National Institutes of Health Guidelines for the Care and Use of Laboratory Animals and conformed to the Code of Practice of the National Health and Medical Research Council of Australia.

CRediT authorship contribution statement

Niliksha Gunewardene: Writing – review & editing, Writing – original draft, Visualization, Validation, Supervision, Software, Resources, Project administration, Methodology, Investigation, Funding acquisition, Formal analysis, Data curation, Conceptualization. **Patrick Lam:** Writing – review & editing, Visualization, Software, Resources, Project administration, Formal analysis, Data curation. **Jiwei Song:** Visualization, Formal analysis, Data curation. **Trung Nguyen:** Data curation. **Shannon Mendez Ruiz:** Data curation. **Raymond C.B. Wong:** Data curation. **Andrew K. Wise:** Writing – review & editing, Writing – original draft, Visualization, Validation, Supervision, Software, Resources, Project administration, Methodology, Investigation, Funding acquisition, Formal analysis, Data curation, Conceptualization. **Rachael T. Richardson:** Writing – review & editing, Writing – original draft, Visualization, Validation, Supervision, Software, Resources, Project administration, Methodology, Investigation, Funding acquisition, Formal analysis, Data curation, Conceptualization.

Declaration of competing interest

The author(s) declare no competing interests.

Acknowledgements

This work was funded with support from Bionics Institute. The Bionics Institute and the Centre for Eye Research Australia acknowledges the support it receives from the Victorian Government, Australia, through its Operational Infrastructure Support Program. The authors would like to thank Flip Kammerer, David Nguyen, Alexander Hill, James Firth, Sayward Barone, Ella Trang and Peta Grigsby from the Bionics Institute, Melbourne, Australia, for technical assistance. The authors would also like to extend their thanks to Prof Edwin Rubel for providing the mouse deafness model.

Supplementary materials

Supplementary material associated with this article can be found, in the online version, at doi:10.1016/j.heares.2024.109170.

Data availability

Data will be made available on request.

References

Adler, H.J., Raphael, Y., 1996. New hair cells arise from supporting cell conversion in the acoustically damaged chick inner ear. Neurosci Lett 205, 17–20.

Atkinson, P.J., Wise, A.K., Flynn, B.O., Nayagam, B.A., Richardson, R.T., 2014. Hair cell regeneration after ATOH1 gene therapy in the cochlea of profoundly deaf adult guinea pigs. PLOS One.

Bermingham, N.A., et al., 1999. Math1: an essential gene for the generation of inner ear hair cells. Science 284, 1837–1841.

Bramhall, N.F., Shi, F., Arnold, K., Hochedlinger, K., Edge, A.S., 2014. Lgr5-positive supporting cells generate new hair cells in the postnatal cochlea. Stem Cell. Rep. 2, 311–322. https://doi.org/10.1016/j.stemcr.2014.01.008.

Cafaro, J., Lee, G.S., Stone, J.S., 2007. Atoh1 expression defines activated progenitors and differentiating hair cells during avian hair cell regeneration. Dev. Dyn. 236, 156–170. https://doi.org/10.1002/dvdy.21023.

Chen, Y., et al., 2016. Histone demethylase LSD1 promotes adipocyte differentiation through repressing Wnt signaling. Cell Chem. Biol. 23, 1228–1240. https://doi.org/10.1016/j.chembiol.2016.08.010.

Chen, Y., et al., 2017. Hedgehog signaling promotes the proliferation and subsequent hair cell formation of progenitor cells in the neonatal mouse cochlea. Front. Mol. Neurosci. 10, 426. https://doi.org/10.3389/fnmol.2017.00426.

Chen, Y., et al., 2021. Generation of mature and functional hair cells by co-expression of Gfi1, Pou4f3, and Atoh1 in the postnatal mouse cochlea. Cell. Rep. 35, 109016. https://doi.org/10.1016/j.celrep.2021.109016.

Corwin, J.T., Cotanche, D.A., 1988. Regeneration of sensory hair cells after acoustic trauma. Science 240, 1772–1774.

Costa, A., et al., 2015. Generation of sensory hair cells by genetic programming with a combination of transcription factors. Development 142, 1948–1959. https://doi.org/10.1242/dev.119149.

Cotanche, D.A., Lee, K.H., Stone, J.S., Picard, D.A., 1994. Hair cell regeneration in the bird cochlea following noise damage or ototoxic drug damage. Anat. Embryol. (Berl.) 189, 1–18.

Cox, B.C., et al., 2014. Spontaneous hair cell regeneration in the neonatal mouse cochlea in vivo. Development 141, 816–829. https://doi.org/10.1242/dev.103036.

Datta, S., et al., 2018. A destabilizing domain allows for fast, noninvasive, conditional control of protein abundance in the mouse eye - implications for ocular gene therapy. Invest. Ophthalmol. Vis. Sci. 59, 4909–4920. https://doi.org/10.1167/iovs.18-24987.

Dogbevia, G.K., Robetamanith, M., Sprengel, R., Hasan, M.T., 2016. Flexible, AAV-equipped genetic modules for inducible control of gene expression in mammalian brain. Mol. Ther. Nucl. Acid. 5, e309. https://doi.org/10.1038/mtna.2016.23.

Eckrich, S., et al., 2019. Cochlea-specific deletion of Ca(v)1.3 calcium channels arrests inner hair cell differentiation and unravels pitfalls of conditional mouse models. Front. Cell Neurosci. 13, 225. https://doi.org/10.3389/fncel.2019.00225.

Fujioka, M., Okano, H., Edge, A.S., 2015. Manipulating cell fate in the cochlea: a feasible therapy for hearing loss. Trend. Neurosci. 38, 139–144. https://doi.org/10.1016/j.tins.2014.12.004.

Georgievska, B., et al., 2004. Regulated delivery of glial cell line-derived neurotrophic factor into rat striatum, using a tetracycline-dependent lentiviral vector. Hum. Gene Ther. 15, 934–944. https://doi.org/10.1089/hum.2004.15.934.

Golub, J.S., et al., 2012. Hair cell replacement in adult mouse utricles after targeted ablation of hair cells with diphtheria toxin. J. Neurosci. 32, 15093–15105. https://doi.org/10.1523/JNEUROSCI.1709-12.2012.

Groves, A.K., 2010. The challenge of hair cell regeneration. Exp. Biol. Med. (Maywood) 235, 434–446. https://doi.org/10.1258/ebm.2009.009281, 235/4/434 [pii].

Gunewardene, N., Guo, X.C., Wong, Y.C.A., Thorne, R.P., Vlajkovic, M.S., 2013. Adenosine amine congener ameliorates cisplatin-induced hearing loss. World J. Otorhinolaryngol.

Henderson, D., Bielefeld, E.C., Harris, K.C., Hu, B.H., 2006. The role of oxidative stress in noise-induced hearing loss. Ear Hear 27, 1–19. https://doi.org/10.1097/01.aud.0000191942.36672.f3.

Hertzano, R., et al., 2004. Transcription profiling of inner ears from Pou4f3(ddl/ddl) identifies Gfi1 as a target of the Pou4f3 deafness gene. Hum. Mol. Genet. 13, 2143–2153. https://doi.org/10.1093/hmg/ddh218.

Holtzman, L., Gersbach, C.A., 2018. Editing the epigenome: reshaping the genomic landscape. Annu. Rev. Genom. Hum. Genet. 19, 43–71. https://doi.org/10.1146/annurev-genom-083117-021632.

Hu, L., et al., 2016. Diphtheria toxin-induced cell death triggers Wnt-dependent hair cell regeneration in neonatal mice. J. Neurosci. 36, 9479–9489. https://doi.org/10.1523/JNEUROSCI.2447-15.2016.

Ikeda, R., Pak, K., Chavez, E., Ryan, A.F., 2015. Transcription factors with conserved binding sites near ATOH1 on the POU4F3 gene enhance the induction of cochlear hair cells. Mol. Neurobiol. 51, 672–684. https://doi.org/10.1007/s12035-014-8801-y.

Isgrig, K., Chien, W.W., 2018. Posterior semicircular canal approach for inner ear gene delivery in neonatal mouse. J. Vis. Exp. https://doi.org/10.3791/56648.

Isgrig, K., et al., 2019. AAV2.7m8 is a powerful viral vector for inner ear gene therapy. Nat. Commun. 10, 427. https://doi.org/10.1038/s41467-018-08243-1.

Ivanova, A., et al., 2005. In vivo genetic ablation by Cre-mediated expression of diphtheria toxin fragment A. Genesis 43, 129–135. https://doi.org/10.1002/gene.20162.

Iwamoto, M., Bjorklund, T., Lundberg, C., Kirik, D., Wandless, T.J., 2010. A general chemical method to regulate protein stability in the mammalian central nervous system. Chem. Biol. 17, 981–988. https://doi.org/10.1016/j.chembiol.2010.07.009.

Iyer, A.A., et al., 2022. Cellular reprogramming with ATOH1, GFI1, and POU4F3 implicate epigenetic changes and cell-cell signaling as obstacles to hair cell regeneration in mature mammals. Elife 11. https://doi.org/10.7554/eLife.79712.

Izumikawa, M., et al., 2005. Auditory hair cell replacement and hearing improvement by Atoh1 gene therapy in deaf mammals. Nat. Med. 11, 271–276. https://doi.org/10.1038/nm1193.

Izumikawa, M., Batts, S.A., Miyazawa, T., Swiderski, D.L., Raphael, Y., 2008. Response of the flat cochlear epithelium to forced expression of Atoh1. Hear Res. 240, 52–56. https://doi.org/10.1016/j.heares.2008.02.007.

Jen, H.I., et al., 2019. Transcriptomic and epigenetic regulation of hair cell regeneration in the mouse utricle and its potentiation by Atoh1. Elife 8. https://doi.org/10.7554/eLife.44328.

Jen, H.I., et al., 2022. GFI1 regulates hair cell differentiation by acting as an off-DNA transcriptional co-activator of ATOH1, and a DNA-binding repressor. Sci. Rep. 12, 7793. https://doi.org/10.1038/s41598-022-11931-0.

Kaur, C., Van Orden, M., O'Malley, J.T., Wu, P.Z., Liberman, M.C., 2023a. Supporting-cell vs. hair-cell survival in the human cochlea: implications for regenerative therapies. Hear Res. 435, 108815. https://doi.org/10.1016/j.heares.2023.108815.

Kaur, C., Van Orden, M., O'Malley, J.T., Wu, P.Z., Liberman, M.C., 2023b. Supporting-cell vs. hair-cell survival in the human cochlea: implications for regenerative therapies. bioRxiv. https://doi.org/10.1101/2023.04.24.538119.

Kelly, M.C., Chang, Q., Pan, A., Lin, X., Chen, P., 2012. Atoh1 directs the formation of sensory mosaics and induces cell proliferation in the postnatal mammalian cochlea in vivo. J. Neurosci. 32, 6699–6710. https://doi.org/10.1523/JNEUROSCI.5420-11.2012, 32/19/6699 [pii].

Kerenyi, M.A., et al., 2013. Histone demethylase Lsd1 represses hematopoietic stem and progenitor cell signatures during blood cell maturation. Elife 2, e00633. https://doi.org/10.7554/eLife.00633.

Kim, Y.H., Raphael, Y., 2007. Cell division and maintenance of epithelial integrity in the deafened auditory epithelium. Cell Cycle 6, 612–619.

Kujawa, S.G., Liberman, M.C., 2009. Adding insult to injury: cochlear nerve degeneration after "temporary" noise-induced hearing loss. J. Neurosci.: Off. J. Soc. Neurosci. 29, 14077–14085. https://doi.org/10.1523/JNEUROSCI.2845-09.2009.

Kurotsu, S., Suzuki, T., Ieda, M., 2017. Direct reprogramming, epigenetics, and cardiac regeneration. J. Card. Fail. 23, 552–557. https://doi.org/10.1016/j.cardfail.2017.05.009.

Lee, S., et al., 2020. Combinatorial Atoh1 and Gfi1 induction enhances hair cell regeneration in the adult cochlea. Sci. Rep. 10, 21397. https://doi.org/10.1038/s41598-020-78167-8.

Lei, Z.J., et al., 2015. Lysine-specific demethylase 1 promotes the stemness and chemoresistance of Lgr5+ liver cancer initiating cells by suppressing negative regulators of beta-catenin signaling. Oncogene 34, 3214. https://doi.org/10.1038/onc.2015.182.

Lenz, D.R., et al., 2019. Applications of Lgr5-Positive Cochlear Progenitors (LCPs) to the Study of Hair Cell Differentiation. Front. Cell Dev. Biol. 7, 14. https://doi.org/10.3389/fcell.2019.00014.

Liu, Z., et al., 2012. Age-dependent in vivo conversion of mouse cochlear pillar and Deiters' cells to immature hair cells by Atoh1 ectopic expression. J. Neurosci. 32, 6600–6610. https://doi.org/10.1523/JNEUROSCI.0818-12.2012.

Liu, Y., et al., 2024. Combinatorial Atoh1, Gfi1, Pou4f3, and Six1 gene transfer induces hair cell regeneration in the flat epithelium of mature guinea pigs. Hear Res. 441, 108916. https://doi.org/10.1016/j.heares.2023.108916.

Lu, N., et al., 2013. Sonic hedgehog initiates cochlear hair cell regeneration through downregulation of retinoblastoma protein. Biochem. Biophys. Res. Commun. 430, 700–705. https://doi.org/10.1016/j.bbrc.2012.11.088.

Lu, Y., et al., 2020. Reprogramming to recover youthful epigenetic information and restore vision. Nature 588, 124–129. https://doi.org/10.1038/s41586-020-2975-4.

Maiques-Diaz, A., Somervaille, T.C., 2016. LSD1: biologic roles and therapeutic targeting. Epigenomics 8, 1103–1116. https://doi.org/10.2217/epi-2016-0009.

Maiques-Diaz, A., et al., 2018. Enhancer activation by pharmacologic displacement of LSD1 from GFI1 induces differentiation in acute myeloid leukemia. Cell. Rep. 22, 3641–3659. https://doi.org/10.1016/j.celrep.2018.03.012.

Mansuy, I.M., et al., 1998. Inducible and reversible gene expression with the rtTA system for the study of memory. Neuron 21, 257–265. https://doi.org/10.1016/s0896-6273(00)80533-4.

McGovern, M.M., Zhou, L., Randle, M.R., Cox, B.C., 2018. Spontaneous Hair Cell Regeneration Is Prevented by Increased Notch Signaling in Supporting Cells. Front. Cell Neurosci. 12, 120. https://doi.org/10.3389/fncel.2018.00120.

McGovern, M.M., et al., 2024. Expression of Atoh1, Gfi1, and Pou4f3 in the mature cochlea reprograms nonsensory cells into hair cells. Proc. Natl. Acad. Sci. U.S.A. 121, e2304680121. https://doi.org/10.1073/pnas.2304680121.

McLean, W.J., et al., 2017. Clonal expansion of Lgr5-positive cells from mammalian cochlea and high-purity generation of sensory hair cells. Cell. Rep. 18, 1917–1929. https://doi.org/10.1016/j.celrep.2017.01.066.

Mizutari, K., et al., 2013. Notch inhibition induces cochlear hair cell regeneration and recovery of hearing after acoustic trauma. Neuron 77, 58–69. https://doi.org/10.1016/j.neuron.2012.10.032. S0896-6273(12)00953-1 [pii].

Muller, F., et al., 2022. CBP/p300 activation promotes axon growth, sprouting, and synaptic plasticity in chronic experimental spinal cord injury with severe disability. PLoS Biol. 20, e3001310. https://doi.org/10.1371/journal.pbio.3001310.

Nadol Jr., J.B., Ketten, D.R., Burgess, B.J, 1994. Otopathology in a case of multichannel cochlear implantation. Laryngoscope 104, 299–303. https://doi.org/10.1288/00005537-199403000-00010.

Nguyen, J.D., et al., 2023. DNA methylation in the mouse cochlea promotes maturation of supporting cells and contributes to the failure of hair cell regeneration. Proc. Natl. Acad. Sci. U.S.A. 120, e2300839120. https://doi.org/10.1073/pnas.2300839120.

Quintino, L., et al., 2013. Functional neuroprotection and efficient regulation of GDNF using destabilizing domains in a rodent model of Parkinson's disease. Mol. Ther. 21, 2169–2180. https://doi.org/10.1038/mt.2013.169.

Quintino, L., et al., 2018. Destabilizing Domains Enable Long-Term and Inert Regulation of GDNF Expression in the Brain. Mol. Ther. Method. Clin. Dev. 11, 29–39. https://doi.org/10.1016/j.omtm.2018.08.008.

Raphael, Y., Altschuler, R.A., 1991. Scar formation after drug-induced cochlear insult. Hear Res. 51, 173–183.

Ryals, B.M., Rubel, E.W., 1988. Hair cell regeneration after acoustic trauma in adult Coturnix quail. Science 240, 1774–1776.

Samarajeewa, A., et al., 2018. Transcriptional response to Wnt activation regulates the regenerative capacity of the mammalian cochlea. Development 145.

Shou, J., Zheng, J.L., Gao, W.Q., 2003. Robust generation of new hair cells in the mature mammalian inner ear by adenoviral expression of Hath1. Mol. Cell. Neurosci. 23, 169–179.

Tai, K., Quintino, L., Isaksson, C., Gussing, F., Lundberg, C., 2012. Destabilizing domains mediate reversible transgene expression in the brain. PLoS One 7, e46269. https://doi.org/10.1371/journal.pone.0046269.

Tao, L., et al., 2021. Enhancer decommissioning imposes an epigenetic barrier to sensory hair cell regeneration. Dev. Cell. 56, 2471–2485. https://doi.org/10.1016/j.devcel.2021.07.003 e2475.

Tong, L., et al., 2015. Selective deletion of cochlear hair cells causes rapid age-dependent changes in spiral ganglion and cochlear nucleus neurons. J. Neurosci. 35, 7878–7891. https://doi.org/10.1523/JNEUROSCI.2179-14.2015.

Verdoodt, D., Peeleman, N., Van Camp, G., Van Rompaey, V., Ponsaerts, P., 2021. Transduction Efficiency and Immunogenicity of Viral Vectors for Cochlear Gene Therapy: a Systematic Review of Preclinical Animal Studies. Front. Cell Neurosci. 15, 728610. https://doi.org/10.3389/fncel.2021.728610.

Wallis, D., et al., 2003. The zinc finger transcription factor Gfi1, implicated in lymphomagenesis, is required for inner ear hair cell differentiation and survival. Development 130, 221–232.

Walters, B.J., et al., 2017. In Vivo Interplay between p27Kip1, GATA3, ATOH1, and POU4F3 Converts Non-sensory Cells to Hair Cells in Adult Mice. Cell. Rep. 19, 307–320. https://doi.org/10.1016/j.celrep.2017.03.044.

Warchol, M.E., 2011. Sensory regeneration in the vertebrate inner ear: differences at the levels of cells and species. Hear Res. 273, 72–79. https://doi.org/10.1016/j.heares.2010.05.004.

Wu, X.N., et al., 2017. Methylation of transcription factor YY2 regulates its transcriptional activity and cell proliferation. Cell Discov. 3, 17035. https://doi.org/10.1038/celldisc.2017.35.

Zeng, H., et al., 2008. An inducible and reversible mouse genetic rescue system. PLoS Genet. 4, e1000069. https://doi.org/10.1371/journal.pgen.1000069.

Zhang, W.J., et al., 2016. Regulation of Transcription Factor Yin Yang 1 by SET7/9-mediated Lysine Methylation. Sci. Rep. 6, 21718. https://doi.org/10.1038/srep21718.

Zhang, J., et al., 2018. ERBB2 signaling drives supporting cell proliferation in vitro and apparent supernumerary hair cell formation in vivo in the neonatal mouse cochlea. Eur J. Neurosci. 48, 3299–3316. https://doi.org/10.1111/ejn.14183.

Zheng, J.L., Gao, W.Q., 2000. Overexpression of Math1 induces robust production of extra hair cells in postnatal rat inner ears. Nat. Neurosci. 3, 580–586. https://doi.org/10.1038/75753.

Zhou, A., et al., 2016. Nuclear GSK3beta promotes tumorigenesis by phosphorylating KDM1A and inducing its deubiquitylation by USP22. Nat. Cell Biol. 18, 954–966. https://doi.org/10.1038/ncb3396.